

- ⁴H. P. Kelly, Phys. Rev. **144**, 39 (1966).
⁵P. W. Langhoff, M. Karplus, and R. P. Hurst, J. Chem. Phys. **44**, 505 (1966).
⁶J. Lahiri and A. Mukherji, J. Phys. Soc. (Japan) **21**, 1178 (1966).
⁷R. P. Feynman, Phys. Rev. **56**, 340 (1939).
⁸E. S. Chang, Ph. D. dissertation, 1967, University of California, Riverside (unpublished).
⁹We wish to thank Professor H. P. Kelly for calling our attention to this point.
¹⁰A more complete list is given in Refs. 3 and 8.
¹¹R. M. Sternheimer, Phys. Rev. **96**, 951 (1954).
¹²A. Salop, E. Pollack, and B. Bederson, Phys. Rev. **124**, 1431 (1961).
¹³G. E. Chamberlain and J. C. Zorn, Phys. Rev. **129**, 677 (1963).
¹⁴A. Dalgarno and R. M. Pengelly, Proc. Phys. Soc. (London) **89**, 503 (1966).
¹⁵G. M. Stacey, Proc. Phys. Soc. (London) **88**, 896 (1966).
¹⁶K. Murakawa and M. Yamamoto, J. Phys. Soc. (Japan) **21**, 821 (1966).
¹⁷The contribution from diagram 1(j) is comparable with that from 1(h) but does not have to be considered specifically in the subsequent discussion because it leads to diagram 2(c) which is identical with that resulting from 1(h). All remarks about the relative importance of 1(h) then apply to 1(j).

Determination of g -Factor Ratios for Free Rb^{85} and Rb^{87} Atoms*

C. W. White,[†] W. M. Hughes, G. S. Hayne, and H. G. Robinson
Duke University, Durham, North Carolina
 (Received 6 May 1968)

The ratio of the nuclear g factor to the electronic g factor in the ground electronic state of free $\text{Rb}^{85,87}$ atoms has been determined using optical pumping techniques in a magnetic field of ≤ 50 G. Typical linewidths were ≤ 15 cps. The linewidth contribution due to magnetic field effects was less than 1 cps. The ratio of electronic g factors for the Rb isotopes was also measured. The results are $-g_I/g_J(\text{Rb}^{87}) = 4.969\,914\,7 \times (1 \pm 0.9 \times 10^{-6}) \times 10^{-4}$, $-g_I/g_J(\text{Rb}^{85}) = 1.466\,490\,8 \times (1 \pm 2.1 \times 10^{-6}) \times 10^{-4}$, and $g_J(\text{Rb}^{87})/g_J(\text{Rb}^{85}) = 1.000\,000\,004\,1 \times (1 \pm 6.0 \times 10^{-9})$. These results were obtained from evacuated wall-coated cells having the Lorentzian line shape. Cells filled with inert buffer gases exhibited small, uncontrollable, systematic error due to non-Lorentzian line shape. In both types of cells, the Zeeman resonances exhibited frequency shifts proportional to the pumping-light intensity. The ratio $g_I(\text{Rb}^{85})/g_J(\text{Rb}^{87}) = 0.295\,073\,6 \times (1 \pm 2.3 \times 10^{-6})$ was obtained by combining the results above. The combination with results of other researchers yields the chemical shift of Rb^+ in aqueous solution relative to the free atom as $\Delta\sigma(\text{Rb}^+_{\text{aq}}/\text{Rb}) = -(211.6 \pm 1.2) \times 10^{-6}$. Absolute values in units of the Bohr magneton for the shielded nuclear moments are derived using only g -factor ratios for free atoms: $g_I(\text{Rb}^{87}) = -0.995\,141\,4 \times 10^{-3} \times (1 \pm 1.0 \times 10^{-6})$ and $g_I(\text{Rb}^{85}) = -0.293\,6400 \times 10^{-3} \times (1 \pm 2.2 \times 10^{-6})$.

I. INTRODUCTION

The basic motivation for this work followed from the desire to measure ground-electronic-state alkali g_J ratios to high precision using optical-pumping techniques incorporating the advantages of wall-coated evacuated cells. Earlier efforts¹ using the Rb isotopes were limited in resolution primarily by the applied magnetic field. The work to be reported in this paper is unique in enjoying a field improved beyond the point where it contributed significantly to the system resolution. In experiments using this improved apparatus, when the then-latest atomic-beam² determination for $g_I/g_J(\text{Rb}^{85})$ was used in the Breit-Rabi equation to fit experimental data, the g_J value derived from $\Delta F=0$ Zeeman transitions in the $F=3$ level complex differed significantly from the value for the $F=2$ level complex. Accordingly, our experiment was

inverted to determine the g_I/g_J ratios for the Rb isotopes. Following publication of preliminary results,³ two other experiments^{4,5} were initiated whose results confirmed our conclusion that the earlier $g_I/g_J(\text{Rb}^{85})$ value was in error. This paper reports the final results for our measurement of g_I/g_J in $\text{Rb}^{85,87}$ and of $g_J(\text{Rb}^{85})/g_J(\text{Rb}^{87})$. The high resolution of the experiment permitted the first observation of shifts in the $\Delta F=0$ Zeeman transitions of Rb induced by the pumping light.

II. THEORY

The energy levels of the $^2S_{1/2}$ electronic state of an alkali atom in an applied magnetic field, \vec{H} , are assumed to be represented by the effective Hamiltonian

$$\mathcal{H} = h a \vec{I} \cdot \vec{J} + g_J \mu_0 \vec{J} \cdot \vec{H} + g_I \mu_0 \vec{I} \cdot \vec{H} \quad (1)$$

where a is a hyperfine interaction constant, and $g_J = -\mu_J/\mu_0 J$ and $g_I = \mu_I/\mu_0 I$ are the electronic and nuclear gyromagnetic ratios respectively. The appropriate values for these "constants" are to be determined by the atom and its environment. Thus without having to write explicit perturbation terms involving excited states, the effect of certain environmental perturbations on the atom can be incorporated into the effective Hamiltonian by using experimentally determined constants (which may differ from those of the free atom).

The various energy levels within the electronic ground state are given by the Breit-Rabi formula. Using $F_+ = I + \frac{1}{2}$ and $F_- = I - \frac{1}{2}$ for the allowed values of the total angular momentum, the frequency of a Zeeman transition ($\Delta F = 0$, $|\Delta m_F| = 1$) is

$$\nu(F_+; m_{F_+} \leftrightarrow m_{F_+} - 1) = \pm g_I \mu_0 H/h + \frac{\Delta\nu}{2} \left[\left(1 + \frac{4m_{F_+}x}{2I+1} + x^2 \right)^{1/2} - \left(1 + \frac{4(m_{F_+}-1)x}{2I+1} + x^2 \right)^{1/2} \right], \quad (2)$$

with $x = (g_J - g_I)\mu_0 H/h\Delta\nu$ where μ_0 is the Bohr magneton, h is Planck's constant, and $\Delta\nu$ is the zero-field hyperfine separation $|(2I+1)a/2|$. The quantities $\mu_0 g_I H/h$ and $\mu_0 g_J H/h$ hereafter will be referred to as ν_I and ν_J respectively. From Eq. (2),

$$\nu_I = \frac{1}{2} \left[\nu(F_+; m_{F_+} \leftrightarrow m_{F_+} - 1) - \nu(F_-; m_{F_-} \leftrightarrow m_{F_-} - 1) \right]. \quad (3)$$

This is then just the resonance frequency of the (shielded) nucleus in the applied magnetic field. For Rb^{87} ($I = 3/2$), there are two such frequency differences which can be used to determine ν_I . For Rb^{85} ($I = 5/2$), there are four such frequency differences.

Since the zero-field hyperfine separation $\Delta\nu$ is known to precision adequate for our case, the Breit-Rabi formula can be viewed as a relation between ν_I , ν_J , and the experimental frequency of a transition of specified F and m_F in the alkali atom of interest. Given measurement of two different transitions then, one has enough information to solve for both ν_I and ν_J at a given magnetic field or, more to the point, to determine the ratio $\nu_I/\nu_J = g_I/g_J$. The mechanics of this process are handled by a simple FORTRAN routine in determining our final experimental results. A useful alternative method involves summing all Zeeman transition frequencies in the upper hyperfine level complex:

$$m_{F_+} = +(I + 1/2) \sum \nu(F_+; m_{F_+} \leftrightarrow m_{F_+} - 1) = \nu_J + 2I\nu_I. \quad (4)$$

$$m_{F_-} = -(I - 1/2)$$

This sum and ν_I from Eq. (3) permit determination of ν_I/ν_J . This alternative method is useful for checking raw data at the time the experiment is being performed; its disadvantage is that more frequencies must be measured, and it was used only as an occasional check of data.

The sign of g_I can be determined using Zeeman transitions only and the Breit-Rabi equation. The simplest case occurs when the magnetic field is low and the quadratic splittings are small. With sufficient resolution, two groups of Zeeman resonances structured by the quadratic splitting are observed when $I > 1/2$. One group corresponds to resonances in the $F_+ = I + 1/2$ level complex; the other, to resonances in the $F_- = I - 1/2$ level complex. If the nuclear g factor is negative, the F_- resonances will be higher in frequency than the F_+ resonances by $2|\nu_I|$. The F_+ and F_- groups can be distinguished by counting the resonances in each. The sign determined in this experiment was consistent with the earlier determination of NMR.⁷

III. APPARATUS

A schematic diagram of the apparatus is shown in Fig. 1. The applied magnetic field was produced by a precision-wound solenoid, 36 in. long and 10 in. i. d., surrounded by a cylindrical nest of three Molypermalloy magnetic shields. Correction coils were provided for compensation of field inhomogeneities. The coils were designed to provide reasonable orthogonality between adjustment of the various coils.⁸ In an applied magnetic field of ~ 50 G, the Rb^{87} Zeeman transition linewidths extrapolated to zero light intensity were ~ 5 parts in 10^7 of the transition frequencies in a 100-cm³ sample buffered with 148-Torr He. This provided a measure of the spatial homogeneity of the magnetic field.

A constant current supply was used to drive the solenoid. The long-term fractional current drift was ≤ 1 part in 10^6 /hr and the short term current noise was ~ 1 part 10^7 . The noise limit was determined by the noise of the feedback amplifier.

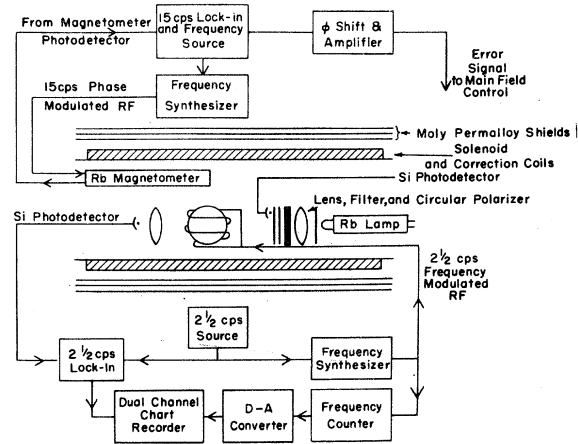


FIG. 1. Schematic diagram of apparatus.

The magnetic field was stabilized by an independent optically pumped Rb magnetometer. The frequency of the strongest Rb⁸⁷ ground-state Zeeman transition was locked to a frequency synthesizer having a stable crystal oscillator for its time base. Phase modulation at a 15-cps rate was used so that the magnetic field itself remained unmodulated. The locked-field fractional stability was better than 2 parts in 10⁸/hr.

The optical-pumping apparatus used Dehmelt's transmission-monitoring technique.⁹ The light source was always operated in the same magnetic field as the sample, and the light was sufficiently stable to allow direct coupling of the signal through the amplifier and lock-in detector. The rf field at the main sample cell was supplied by a frequency synthesizer which could be either frequency-modulated or amplitude-modulated (AM) at the rate of 2.5 cps. The Si-photodetector signal at this frequency was amplified and fed to a lock-in detector whose output was displayed on a chart recorder. The frequency was determined by counting over a 10-sec period. A digital-to-analog converter was used to record the frequency on the second channel of the chart recorder.

Both evacuated wall-coated¹⁰ cells and cells filled with various pressures of He or Ne buffer gas were used. Parafilm-type RG,¹¹ tetracontane, dotriacontane, and eicosane wall coatings were used in evacuated cells with volumes of 100 or 200 cm³. The wax was applied either by introduction directly on the wall or by evaporation from a heated wax carrier at the center of the cell. Rb metal was located in a side arm and entered the cell volume through an aperture ≤ 1 mm in diameter.¹² At a resonance frequency of ~ 36 Mc/sec, Rb⁸⁷ linewidths extrapolated to zero light intensity were between 5 and 14 cps depending on the particular cell used. Linewidths for cells with the same geometry and wall-coating material were not the same. Experimental evidence indicates that the linewidth of most of the wall-coated cells was dominated by wall relaxation. In such cells, the (motionally narrowed) linewidth due to magnetic field inhomogeneity was apparently ≤ 1 cps. Figure 2 shows typical AM line shapes obtained in the two types of cell. The indicated points represent a Lorentzian fit to each curve.

IV. PROCEDURE

With the applied magnetic field locked to a stable frequency, the inhomogeneity correction coils were adjusted by observing the strongest Rb⁸⁷ resonance on an oscilloscope. When a buffer-gas cell was in use, the line shape and linewidth were sensitive functions of the coil settings. Final adjustment was made by recording the (AM) line shape and adjusting the shims for optimum line symmetry. For buffered cells this criterion was adopted in preference to maximizing signal height or minimizing linewidth. With wall-coated cells, optimum linewidth was not a sensitive function of the settings of the correction coils, and line shapes were well represented by a Lorentzian curve.

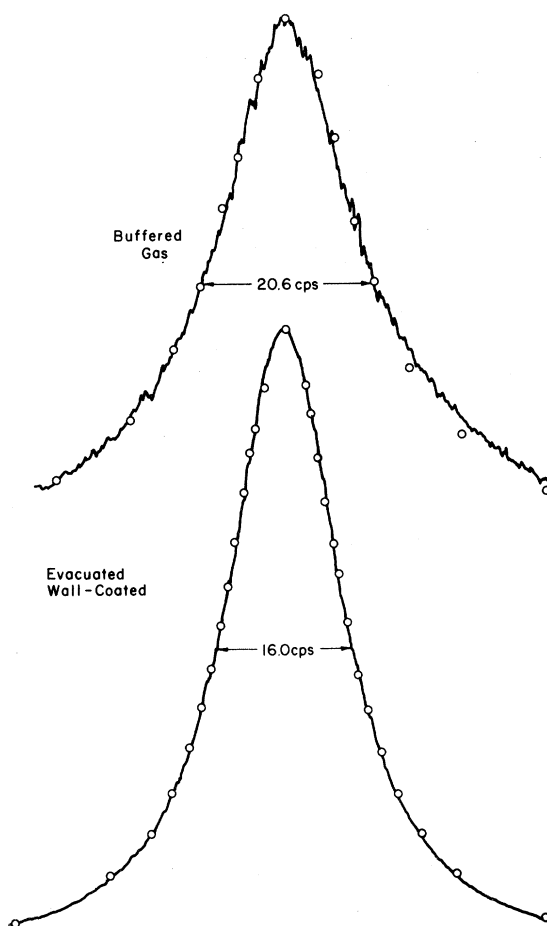


FIG. 2. Rb⁸⁷ experimental line shapes in buffer gas and evacuated wall-coated cells. The points represent a least-squares fit to a Lorentzian line shape.

Data for determination of resonance line centers were taken by using the chart recorder to obtain the FM signal amplitude at several discrete frequencies in the line-center region. After the run was completed, the line-center frequency was determined from a displacement-versus-frequency plot. The discrete-frequency recording technique avoids possible phase shifts incurred by continuous tuning through the resonance. The measurement of a typical pair of Zeeman-resonance line centers to ± 0.15 cps required ~ 5 min. Repetitive measurements were made by alternating successively between the two transitions being investigated. Typically, four line-center determinations per transition were made at a given light intensity and sense of polarization. This procedure was repeated for at least four light intensities. In this way extrapolation to zero light intensity was eventually possible. The series of measurements was repeated for all pairs of transitions which had a sufficient signal-to-noise ratio. Finally, the measurement program was conducted at each of the two senses of circular polarization available in the optical pumping light.

V. RESULTS

A. Measurement of g_I/g_J ($\text{Rb}^{85,87}$)

As an example of typical data, Fig. 3 shows the g_I/g_J ratio as a function of an arbitrary measure of the incident light intensity for Rb^{87} in the 100-cm^3 evacuated, Parafilm wall-coated sample A. For the sake of clarity, only one of the two possible Rb^{87} , ν_I frequency differences at a given polarization of incident light is plotted. The Rb lamp and the absorption cell both contained Rb of natural isotopic abundance and were in the same applied magnetic field of 50 G. The incident light intensity was monitored by a Si photodetector positioned to intercept a portion of the light beam incident on the sample (see Fig. 1). In this paper, the sense of circular polarization is defined to be plus or minus if the selection rule appropriate to the absorption of the pumping light is $\Delta m_F = +1$ or -1 , respectively.

The Hamiltonian of Eq. (1), and the transition frequency it implies, Eq. (2), does not include possible perturbations caused by the incident pumping light. In analyzing the experimental data with this (incomplete) Hamiltonian, each Zeeman transition exhibited a different frequency shift, linear with light intensity. The frequency difference between appropriate pairs of transitions used to determine ν_I was therefore a function of

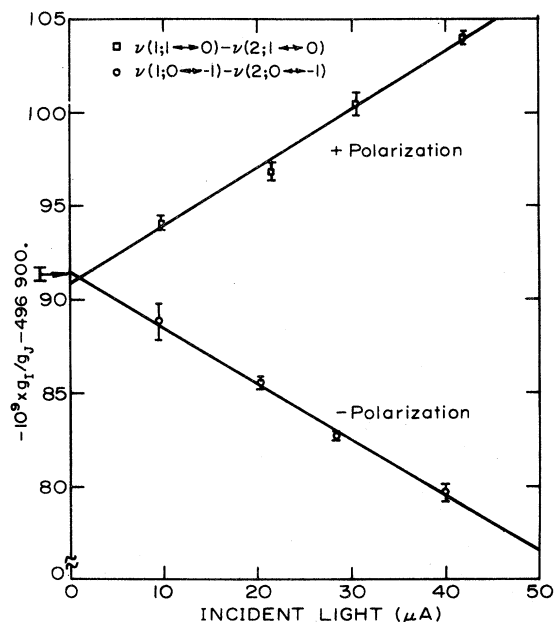


FIG. 3. Measured g_I/g_J (Rb^{87}) as a function of incident light intensity in 100-cm^3 evacuated Parafilm cell A at 50 G. Straight lines are least-squares fitted to the experimental points. Both cell and lamp contain Rb of natural isotopic abundance. The arrow and accompanying error bar represent the weighted mean of all wall-coated-cell extrapolated data and its weighted rms deviation.

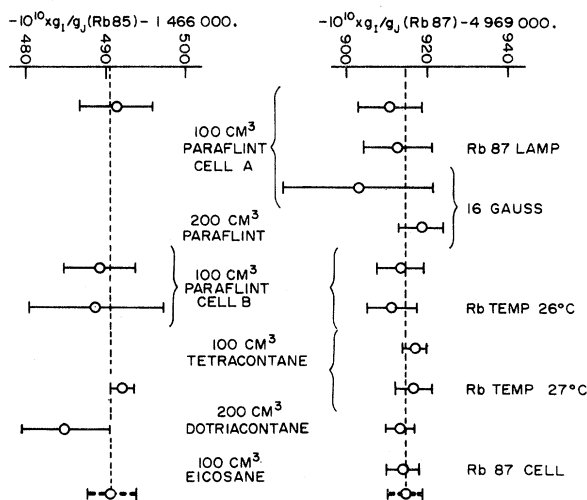


FIG. 4. Summary of g_I/g_J (Rb) results after extrapolation to zero light intensity in evacuated wall-coated cells. Data were taken at 50 G, at a temperature of 35°C , and with natural-abundance Rb in both cell and lamp unless otherwise noted. Error bars represent weighted rms deviations. Dotted lines refer to weighted means quoted in the text.

the incident light intensity. In Fig. 3, after using a least-squares fit to a straight line, the results of extrapolation to zero light intensity were consistent at both senses of polarization. Such extrapolations were in good agreement with the weighted average of all wall-coated-cell extrapolated data, indicated by the arrow. The error bar accompanying the arrow represents the weighted rms deviation of all such extrapolated results.

In computing the weighted over-all average for all extrapolations for a given isotope in the evacuated cells, a weighting factor proportional to the inverse square of the uncertainty of each extrapolation was used. This same weighting factor was used in obtaining the weighted rms deviation for these data. The dashed lines in Fig. 4 refer to these weighted over-all averages plus and minus their respective weighted rms deviations. As an additional check for possible systematic error, a weighted average was computed for each different run (see Fig. 4).

A new run was begun whenever the sample, the light source polarization, temperature of the Rb reservoir, or magnitude of the applied magnetic field was changed. For evacuated cells, no systematic errors were indicated in g_I/g_J determinations following various gross changes in the history of the magnetic field. Unless otherwise stated in Fig. 4, the data were taken in an applied field of 50 G at a Rb reservoir temperature of 35°C using Rb of natural isotopic abundance in both cell and lamp. In comparison with the Rb^{85} case, a relatively large amount of data were taken for Rb^{87} in probing for possible systematic error.

The error associated with the weighted average of each run was found by first obtaining the deviation of unit weight, σ_i , for each extrapolation

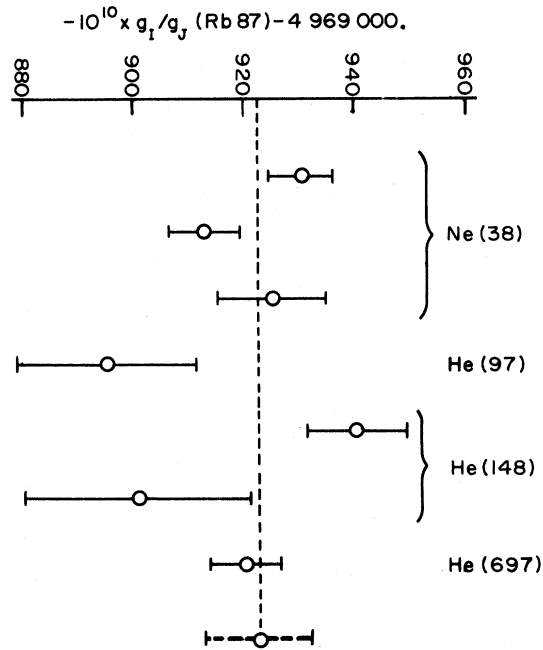


FIG. 5. Summary of g_I/g_J (Rb^{87}) results after extrapolation to zero light intensity in cells filled with buffer gas. Pressure in Torr is indicated in parenthesis. Error bars represent weighted rms deviations. Dotted lines refer to the weighted mean.

in the run: $\sigma_i^2 = U_i^2 + (X_i - \bar{X})^2$. The quantity U_i is the uncertainty in the extrapolated value X_i , and $(X_i - \bar{X})$ represents the deviation of the i th extrapolated value from the weighted average of the run. The weighted deviation of the run was obtained as $\sigma_R^2 = \sum w_i \sigma_i^2$, with w_i the normalized weighting factor proportional to U_i^{-2} . In Fig. 4 the error bars associated with the weighted averages of each run represent $\pm \sigma_R$. We found no evidence for significant systematic error between the various runs.

After finding that our value for g_I/g_J (Rb^{85}) differed from the then-latest atomic-beam value² by about eight times the combined errors, we decided to use uncoated cells filled with buffer gas for a check of gross systematic error in our work. Again, extrapolation to zero light intensity was required. The scatter in the extrapolated results for buffered cells was relatively large primarily because of the sensitivity of the line shape to the magnetic field inhomogeneity. Figure 5 shows results for g_I/g_J (Rb^{87}) for various runs in cells filled with buffer gas. A run was begun each time the field was reshimmied to produce a "symmetric" line shape. Again data were taken in a field of 50 G, at a temperature of 35°C, using natural-isotopic-abundance Rb in both cell and lamp.

The weighted average of the buffered-cell data was higher than the weighted average of the wall-coated-cell data for both isotopes. However, the difference was within the overlap of the weighted

rms deviations. Furthermore, in the buffered cells, the derived value of g_I/g_J was dependent on the type of field gradient present during the run. This is illustrated in the Rb^{87} data in Fig. 5 for the cells buffered with 148-Torr He and 38-Torr Ne. In these samples the history of the field was changed prior to the beginning of each run, and the apparent shifts in g_I/g_J were attributed to the dependence of the line shape on the magnetic field gradients. Hence, with the resolution of this experiment, an inherent inability to avoid small systematic errors in buffer-cell data was suspected.

Because of the larger scatter and the implication of systematic error due to field gradients in the buffered-cell data, a final result was quoted in terms of the results of the evacuated-cell runs only. The weighted average and weighted rms deviation of the g_I/g_J ratio for the free $\text{Rb}^{85, 87}$ atoms for the evacuated cell runs were

$$-g_I/g_J(\text{Rb}^{87}) = 4.9699147 \times (1 \pm 0.9 \times 10^{-6}) \times 10^{-4},$$

$$-g_I/g_J(\text{Rb}^{85}) = 1.4664908 \times (1 \pm 2.1 \times 10^{-6}) \times 10^{-4}.$$

Histograms depicting the g_I/g_J determination for each extrapolation in the wall-coated cells are shown in Fig. 6. Equal weighting of each determination was used in plotting these figures, but the weighted average and weighted rms deviation are indicated at the top of each histogram.

The result for Rb^{85} is in disagreement with the atomic-beam measurement of Penselin *et al.*² Although the beam experiment was conducted in a magnetic field of ~ 560 G, while our experiment used ~ 50 G, we know of no theoretical reason for the discrepancy due to the magnitude of the magnetic field. In a recent Rb^{85} atomic-beam experiment, Ehlers *et al.*⁵ reported $g_I/g_J(\text{Rb}^{85})|_{\text{EFS}}$

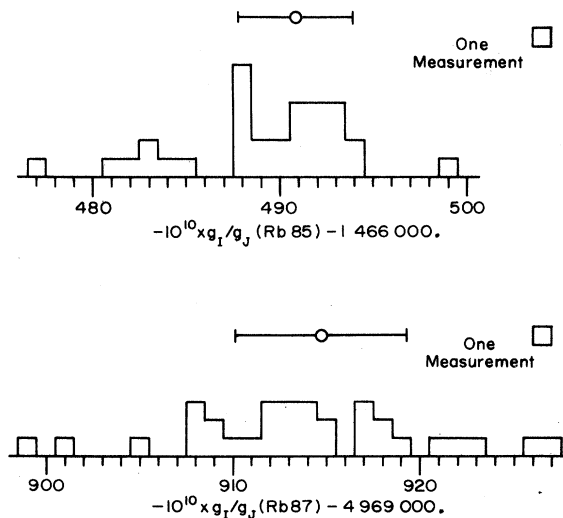


FIG. 6. Histograms of wall-coated-cell results using equal weighting for each extrapolation. The weighted mean and weighted rms deviation are shown at the top of each plot.

$= -1.466478(22) \times 10^{-4}$. Balling,⁴ in an optical pumping experiment, measured the g_I/g_J ratios of Rb⁸⁵,⁸⁷ in He and Ne buffer-gas cells

$$\begin{aligned} g_I/g_J(\text{Rb}^{85})|_B &= -1.46648(8) \times 10^{-4}, \\ g_I/g_J(\text{Rb}^{87})|_B &= -4.96997(9) \times 10^{-4} \end{aligned} \quad (5)$$

These two experiments agree with our reported preliminary results³ as well as with our present results to within the quoted errors.

B. Measurement of $g_J(\text{Rb}^{87})/g_J(\text{Rb}^{85})$

The ratio of $g_J(\text{Rb}^{87})/g_J(\text{Rb}^{85})$ was measured as a function of light intensity in evacuated wall-coated cells and in buffered cells. The ratio was determined at both senses of light polarization from the ν_J values of the following pairs of Zeeman transitions: Rb⁸⁵ (3; 0 \leftrightarrow -1), Rb⁸⁷ (2; 0 \leftrightarrow -1); and Rb⁸⁵ (3; +1 \leftrightarrow 0), Rb⁸⁷ (2; +1 \leftrightarrow 0). In evacuated cells, the value of the free-atom g_J ratio extrapolated to zero light intensity was $g_J(\text{Rb}^{87})/g_J(\text{Rb}^{85}) = 1.000000041 \times (1 \pm 6.0 \times 10^{-9})$. The weighted rms deviation of the four extrapolated results was 5.7×10^{-9} . The uncertainty in the g_J ratio due to the error in the g_I/g_J ratio of the two isotopes was 2×10^{-9} . The over-all error quoted represents the quadratic combination of the weighted rms deviation and the uncertainty in the g_j ratio due to the error in g_I/g_J . The result for the two isotopes of Rb in the buffer-gas cells agreed with that of the evacuated wall-coated cells, but were accurate only to $\pm 1 \times 10^{-8}$. Less precise determinations^{1,13,14} are consistent with the value of this experiment. In the wall-coated cells, if instead of extrapolation to zero light intensity a simple averaging of the data for the two polarizations at one light intensity had been used, an error of 4 parts in 10^8 could have resulted.

C. Determination of $g_I(\text{Rb}^{85})/g_I(\text{Rb}^{87})$

By combining the measured ratio of electron g_J factors with the measured g_I/g_J ratios of the two Rb isotopes, the ratio $g_I(\text{Rb}^{85})/g_I(\text{Rb}^{87})$ for free atoms was derived as

$$\begin{aligned} \frac{g_I(\text{Rb}^{85})}{g_I(\text{Rb}^{87})} &= \frac{g_I/g_J(\text{Rb}^{85})}{g_I/g_J(\text{Rb}^{87})} \times \frac{g_J(\text{Rb}^{85})}{g_J(\text{Rb}^{87})} \\ &= 0.2950736 \times (1 \pm 2.3 \times 10^{-6}) \end{aligned}$$

This ratio should be independent of the chemical environment and therefore can be compared with an NMR determination of the same quantity¹⁵:

$$\begin{aligned} g_I(\text{Rb}^{85})/g_I(\text{Rb}^{87})|_{\text{BEK}} &= 0.2950738 \\ &\times (1 \pm 1.6 \times 10^{-6}). \end{aligned}$$

The agreement is seen to be excellent.

D. Shielding of the Nuclear Moment

Since the value of g_I/g_J determined in this experiment is that for a free atom, appropriate comparison with the nuclear g factor determined by NMR allows evaluation of the relative chemical shift. The ratio of the nuclear g factor for Rb⁺ in an aqueous solution of RbCl and that for the free atom was obtained by using the ratio combinations as follows

$$\begin{aligned} \frac{g_I(\text{Rb}^{+87})}{g_I(\text{Rb}^{87})} &= \frac{g_I(\text{Rb}^{+87})}{g_I(\text{D}_2\text{O})} \frac{g_I(\text{D}_2\text{O})}{g_I(\text{H}_2\text{O})} \frac{g_I(\text{H}_2\text{O})}{g_J(\text{H})} \\ &\times \frac{g_J(\text{H})}{g_J(\text{Rb}^{85})} \frac{g_J(\text{Rb}^{85})}{g_J(\text{Rb}^{87})} \frac{g_J(\text{Rb}^{87})}{g_I(\text{Rb}^{87})} \end{aligned}$$

The values used in addition to the results of this paper were¹⁵⁻¹⁸

$$\begin{aligned} \left| \frac{g_I(\text{Rb}^{+87})}{g_I(\text{D}_2\text{O})} \right| &= 2.1315984 \times (1 \pm 1 \times 10^{-7}), \\ \left| \frac{g_I(\text{D}_2\text{O})}{g_I(\text{H}_2\text{O})} \right| &= 0.153506083 \times (1 \pm 4 \times 10^{-7}), \\ \left| \frac{g_J(\text{H})}{g_J(\text{H}_2\text{O})} \right| &= 658.21591 \times (1 \pm 7 \times 10^{-8}), \\ \left| \frac{g_J(\text{Rb}^{85})}{g_J(\text{H})} \right| &= 1.0000236 \times (1 \pm 1 \times 10^{-7}). \end{aligned} \quad (6)$$

We find for the Rb⁸⁷ isotope:

$$\left| \frac{g_I(\text{Rb}^{+})}{g_I(\text{Rb})} \right| = 1 + (238.2 \pm 1.0) \times 10^{-6}.$$

Similarly, the result for the Rb⁸⁵ isotope is $1 + (239.9 \pm 2.2) \times 10^{-6}$. This implies that $\Delta\sigma(\text{Rb}^{+}_{\text{aq}}/\text{Rb}) = -(238.2 \pm 1.0) \times 10^{-6}$ is the chemical shift of Rb⁺ in an aqueous saturated solution of RbCl relative to the free atom. (The negative sign indicates that the shielding of the nucleus of the free atom is greater than that of the ion in water solution.)

Recently, Lutz¹⁹ has determined alkali nuclear g factors in aqueous solutions extrapolated to zero concentration of the salt. His result for Rb⁸⁷ was

$$\left| \frac{g_I(\text{Rb}^{+87})}{g_I(\text{D}_2\text{O})} \right|_{\text{L}} = 2.1315419 \times (1 \pm 7 \times 10^{-7}).$$

This implies that the chemical shift of Rb⁺⁸⁷ in D₂O relative to the free atom is $\Delta\sigma(\text{Rb}^+_{\text{aq}}/\text{Rb}) = -(211.6 \pm 1.2) \times 10^{-6}$. Since the shielding of the free Rb⁺ ion and that of the free Rb atom are essentially the same,^{20,21} a comparison with the value calculated by Ikenberry and Das²² is possible:

$$\Delta\sigma(\text{Rb}^+_{\text{aq}}/\text{Rb}^+) \Big|_{\text{ID}} = -0.65 \times 10^{-4}. \quad (7)$$

Thus the nucleus of the ion in solution suffers considerably less shielding than the calculated value would indicate.

E. Nuclear g Factor

An absolute value for the Rb nuclear *g* factor was found by forming the product

$$g_I(\text{Rb}) = \frac{g_I(\text{Rb})}{g_J(\text{Rb})} \frac{g_J(\text{Rb})}{g_J(\text{H})} \frac{g_J(\text{H})}{g_I(\text{H})} g_I(\text{H}).$$

The values used for terms not yet listed were²³

$$\left| \frac{g_J(\text{H})}{g_I(\text{H})} \right| = 658.21049 \times (1 \pm 0.30 \times 10^{-6}),$$

$$g_I(\text{H}) = g_p(1 - \alpha^2/3)$$

with^{23, 24}

$$g_p = 3.0420652 \times (1 \pm 2.96 \times 10^{-7}) \times 10^{-3},$$

$$\alpha = 1/137.0359 \times (1 \pm 2 \times 10^{-6}).$$

We note that the *g*-factor ratios required have all been determined for free atoms. The results for the (shielded) nuclear *g* factor of the free Rb atom in terms of the Bohr magneton, μ_B , were

$$g_I(\text{Rb}^{87}) = -0.9951414 \times (1 \pm 1.0 \times 10^{-6}) \times 10^{-3},$$

$$g_I(\text{Rb}^{85}) = -0.2936400 \times (1 \pm 2.2 \times 10^{-6}) \times 10^{-3}.$$

VI. POSSIBLE ERRORS DUE TO SYSTEMATIC FREQUENCY SHIFTS

A. hfs Effect

The question can be raised of a possible systematic error in g_I/g_J caused by a shift in the hfs due to interaction between the "free" atom and the wall. Using $\Delta F=0$ Zeeman transitions alone, it is possible to deduce a value for the hyperfine-interaction constant consistent with the Hamiltonian of Eq. (1). For the evacuated cells of this experiment, using the difference between two adjacent Zeeman-transition frequencies, the hyperfine separation $\Delta\nu(\text{Rb}^{87})$ was determined to a fractional accuracy of 6 parts in 10^7 and $\Delta\nu(\text{Rb}^{85})$ to 3 parts

in 10^7 . Agreement with published hfs values² was obtained, and our results were calculated using the published hfs values. In addition, Brewer²⁵ has measured $\Delta\nu(\text{Rb}^{87})$ in an evacuated cell of 50-ml volume with Paraflint wall coating and found a shift of -1.2 parts in 10^8 . If $\Delta\nu$ were not corrected for this shift, the g_I/g_J ratio calculated from Eq. (2) would be changed by <6.5 parts in 10^{11} . Thus the g_I/g_J results for the 50-G field were particularly insensitive to the change in $\Delta\nu$ caused by the wall coating.

B. Spin-Exchange Effects

A decrease of 9°C in the temperature of the Rb reservoir of one of the Paraflint-coated cells resulted in a decrease in Rb density of $\sim 1/3$ and was accompanied by a linewidth reduction of 1.3 cps. Assuming that the decrease in width was entirely due to spin exchange, the calculated upper limit to the linewidth caused by spin exchange was 4 cps at normal operating temperature. If spin-exchange shifts in Zeeman transitions are proportional to the sense and magnitude of the Rb electron polarization, extrapolation to zero light intensity should remove possible systematic spin-exchange shifts. Not only should the average of these shifts for the two polarizations be zero, but also the magnitude of the shift should approach zero as the polarization goes to zero at zero light intensity. We found no experimental evidence for spin-exchange shifts in the extrapolated values of g_I/g_J .

C. Light-Intensity Effect

The frequency shifts of the ground-state Zeeman transitions which were observed in this experiment were believed to be caused by virtual optical transitions due to nonresonant pumping light incident on the cell. Shifts due to this effect were treated theoretically by Barrat and Cohen-Tannoudji²⁶ and experimentally observed in the ground-state hyperfine transitions of Rb⁸⁷ and Cs¹³³²⁷ and in the ground-state Zeeman transitions of He³²⁸ and Hg¹⁹⁹²⁹. The magnitude of the light-induced hyperfine shift of Rb⁸⁵ and Cs¹³³ was ~ 100 cps, while the magnitude of the shift of the Zeeman transitions observed in this experiment was, at most, a few cycles. Figure 7 shows the measured frequency shifts at the indicated light intensity of some of the Zeeman transitions for Rb^{85, 87} in the 100-cm³ Paraflint wall-coated cell A.

The Zeeman frequency shift as a function of light intensity and polarization is attributed to virtual optical transitions rather than to spin exchange for the following reasons: A reduction in the Rb density by 1/3 did not significantly affect the observed shifts; these shifts were not in general symmetric upon change of polarization; and the shifts were nearly the same at 16 as at 50 G. In buffer-gas samples, the shift decreased with increased pressure and was less than that in evacuated cells.

In addition to light shifts due to virtual optical transitions, a second type of light shift has been treated theoretically²⁶ and observed experimental-

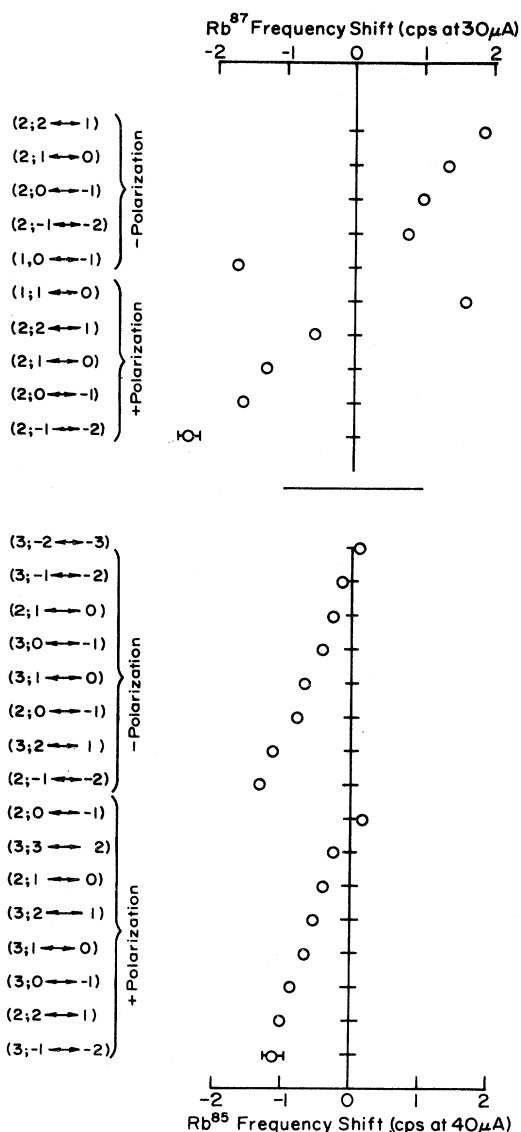


FIG. 7. Frequency shifts of Rb Zeeman transitions caused by the pumping light. An evacuated wall-coated cell was used with both cell and lamp in a 50-G magnetic field. An arbitrary measure of incident light intensity in μA photocurrent was used. Transitions are labeled by $(F; m_F \leftrightarrow m_F - 1)$. Error bars shown apply to all points.

ly.³⁰ This shift involves real optical transitions in which part of the coherence is conserved through the entire optical pumping cycle by the simultaneous optical excitation from two adjacent ground-state Zeeman levels to the excited state and return to the ground state. The shift depends on the light intensity and also on the applied magnetic field through its predicted dependence on the difference of the Larmor frequency in the excited state and in the ground state. The absence of a linear dependence of the shifts on magnetic field

led to the conclusion that the light shifts observed in this experiment were associated with the virtual rather than the real optical transitions.

D. Error Due to Arbitrary Zero of Incident-Light Intensity

The light incident on the cell was monitored by placing a Si photocell in front of the cell. This arbitrary measurement of intensity introduced a small error, $\sim 1 \mu\text{A}$, in the zero of intensity used on each extrapolation. This resulted from a component of light which was not effective in the optical pumping of Rb but which was seen by the incident detector. The effect would be to cause the extrapolations corresponding to plus and minus polarizations not to coincide at zero light intensity. The method of treatment of data discussed in Sec. V explicitly includes any error due to this effect.

E. Lamp Spectral-Profile Effect

In the 100-cm³ Paraflint wall-coated cell A, changing the lamp source from a natural Rb lamp to a lamp of 99.5% Rb⁸⁷ isotopic purity produced no significant shift in g_I/g_J (Rb⁸⁷). This provided an experimental check of the expectation that extrapolation to zero light intensity removes such causes of systematic error.

F. Inhomogeneous-Magnetic-Field Effects

In buffer-gas cells only, shifts of several cps in the Rb⁸⁵ and Rb⁸⁷ Zeeman frequencies at 50 G were observed as a function of the magnitude of the applied rf field, H_1 . The shifts were observed when using rf coils cemented directly to the cell, and the absence of these shifts in the wall-coated cells indicated that the effect was not a Bloch-Siegert³¹ or related effect. The shift was due to inhomogeneities simultaneously present in both H_1 and H_0 . Each Zeeman transition had a different shift and the magnitude of the shift was changed by changing the currents in the inhomogeneity correction coils. A change in the design of the rf coil to improve the spatial homogeneity of the rf magnetic field reduced the magnitude of the shifts to $\leq 1 \times 10^{-8}$ of the transition frequency in the buffer-gas cells.

The use of evacuated wall-coated cells provided unique advantages over buffered cells. In the evacuated cells, it was possible to obtain significant motional averaging of the magnetic field so that the effective homogeneity was greatly increased compared to that for a cell of the same volume filled with buffer gas. In addition, the motional averaging of inhomogeneities guaranteed that the observed line shape was essentially Lorentzian^{32, 33} so that the line center was clearly defined. This becomes particularly important in precision experiments where a line center is to be chosen to some small fraction of the linewidth. For Zeeman transitions, the linewidth³² of the Lorentzian line shape due to the magnetic field inhomogeneity is

$$\delta\omega \approx \gamma^2 \langle (\Delta\vec{B})^2 \rangle_{\text{Vol}}^{1/2} \tau, \quad (8)$$

where γ is the gyromagnetic ratio, $\Delta\vec{B} = \vec{B} - \langle\vec{B}\rangle$ is the deviation of the field from the average field over the cell volume, τ is the correlation time appropriate to the system, and $\langle \rangle_{\text{vol}}$ denotes the average over the sample volume. The condition of applicability of Eq. (8) is that

$$|\gamma| \langle (\Delta\vec{B})^2 \rangle_{\text{vol}}^{1/2} \tau \ll 1. \quad (9)$$

When Eq. (9) is satisfied, inhomogeneity correction coils designed to produce essentially orthogonal magnetic field gradients can be adjusted with little or no interaction between different coils. Thus the adjustments themselves become orthogonal.⁸

Uncontrollable systematic errors were found in buffered cells because of a non-Lorentzian line shape caused by magnetic field inhomogeneities. No such effect was evident in evacuated wall-coated cells even when the linewidth due to magnetic field inhomogeneity was increased by a factor greater than 10 times its normal value. (The over-all linewidth was doubled.) Thus strong experimental and theoretical arguments exist in favor of using the wall-coated evacuated cell.

G. Line-Pulling Effect

There was the possibility of a Zeeman frequency shift due to a variation of the rf power with frequency. A monotonic variation of the rf power with frequency over the range of frequencies for which there is a resonance response will induce a rf pulling effect. Assume that the signal S for the rf field of magnitude H_1 can be written as

$$S = K_1 H_1^2 / [1 + (T_2 \Delta\omega)^2 + K_2 H_1^2]. \quad (10)$$

In the above expression, T_2 is the Bloch spin decorrelation time, K_1 and K_2 are normalizing constants, and $\Delta\omega$ is the frequency difference between the driving frequency ω and the resonant frequency ω_0 . A monotonic variation of rf power with frequency of the form $H_1^2 = h_1^2 [1 \pm |a| \Delta\omega]$ will introduce asymmetry in the line shape and cause a shift $\Delta\omega_s$ of the center frequency

$$\Delta\omega_s = \pm [-1/|a| + (1/a^2 + 1/T_2^2)^{1/2}]. \quad (11)$$

In the above expression the (+) sign refers to a positive slope of rf power versus frequency. For the case when $T_2 \gg |a|$, the above expression reduces to

$$\Delta\omega_s = \pm |a|/2T_2^2. \quad (12)$$

Typical values observed in this experiment were $T_2 \geq 10 \times 10^{-3}$ sec and $|a| \approx 3 \times 10^{-8}$ sec. Using these values, the magnitude of the shift to be expected because of a monotonic frequency-dependent rf power was $\Delta\omega_s \leq 2.5 \times 10^{-5}$ cps. A shift of this order of magnitude could not have been detected in this experiment.

A well-known form of line pulling involves the coupling of the atom to a tuned circuit or cavity. The shift discussed above is fundamentally different and occurs when the driving rf is derived from a nonresonant structure, e.g., a terminated transmission line.

VII. CONCLUSIONS

Optical pumping techniques have been used to conduct precision g_J -ratio and g_I/g_J -ratio experiments on the Rb⁸⁵,⁸⁷ isotopes. In buffer-gas cells, systematic errors caused by magnetic field inhomogeneities were demonstrated. No such effect was evidenced in evacuated wall-coated cells even under conditions where the linewidth due to magnetic field inhomogeneities was increased by a factor >10 times the normal value. Evidence is presented in favor of the use of evacuated wall-coated cells instead of buffered cells where possible. The interaction of the Rb atom with the confining walls was sufficiently small to have no significant effect on the measurements reported. For precision determination of atomic constants using optical pumping techniques, the necessity of extrapolation of data to zero light intensity was clearly demonstrated because of light-induced shifts in the Zeeman transition frequencies. Considerable improvement in precision appears to be possible by obvious extensions of the techniques. Excellent agreement was obtained between appropriate results of this experiment and those of NMR. The g_I/g_J (Rb⁸⁵) value is in agreement with the recent atomic-beam value.⁵

The low value of magnetic field available in this work coupled with the observation of only $\Delta F = 0$ Zeeman transitions precluded a severe test of the Breit-Rabi formula. Nevertheless, the agreement between calculated and observed frequencies (for transitions other than those used in g_I/g_J determinations) was in general ~ 5 parts in 10^9 . A comparison between atomic constants obtained from low-magnetic-field determinations and those obtained at higher values of the magnetic field should permit a more interesting check on deviations from the Breit-Rabi formula.³⁴

*This work was supported in part by U. S. Office of Naval Research and U. S. Army Research Office-Durham. The initial phase of the research enjoyed the support of the National Science Foundation and the National Aeronautics and Space Administration through the Sustaining University Program.

†Present address: Bell Telephone Laboratories, Whippany, New Jersey.

¹G. S. Hayne, E. S. Ensberg, and H. G. Robinson, Phys. Rev. **171**, 20 (1968).

²S. Penselin, T. Moran, V. W. Cohen, and G. Winkler, Phys. Rev. **127**, 524 (1962).

³Preliminary results of this experiment were reported at the Physics of Free Atoms Conference (Berkeley, California, September 12-14, 1966) and at the October 17-19, 1966 meeting of the National Academy of Science

- (Durham, North Carolina) by H. G. Robinson, C. W. White, and G. S. Hayne [see *Science* **21**, 13 (1966)]. Later results were presented by C. W. White, W. M. Hughes, G. S. Hayne, and H. G. Robinson, *Bull. Am. Phys. Soc.* **12**, 507 (1967).
- ⁴L. C. Balling, *Phys. Rev.* **163**, 114 (1967).
- ⁵V. J. Ehlers, T. R. Fowler, and H. A. Shugart, *Phys. Rev.* **167**, 1062 (1968).
- ⁶N. F. Ramsey, *Molecular Beams* (Oxford University Press, Oxford, 1956), Chap. III.
- ⁷See, for example, I. Lindgren, *Arkiv. Fysik* **29**, 553 (1965).
- ⁸C. W. White and H. G. Robinson, *Bull. Am. Phys. Soc.* **11**, 403 (1966).
- ⁹H. G. Dehmelt, *Phys. Rev.* **105**, 1487 (1957).
- ¹⁰H. G. Robinson, E. S. Ensberg, and H. G. Dehmelt, *Bull. Am. Phys. Soc.* **3**, 9 (1958); D. Kleppner, N. F. Ramsey, and P. Fjelstad, *Phys. Rev. Letters* **1**, 232 (1958); H. M. Goldenberg, D. Kleppner, and N. F. Ramsey, *Phys. Rev.* **123**, 530 (1961).
- ¹¹Parafint RG is the commercial name for a mixture of saturated hydrocarbons having between 50 and 55 carbon atoms per molecule, according to the manufacturer. A generous sample of this was supplied to us by Moore and Munger, Inc., 33 Rector Street, N.Y., N.Y.
- ¹²The eicosane-coated cell was of somewhat different geometry than the rest of the cells. We are indebted to P. L. Bender for loaning us this particular cell.
- ¹³K. D. Böklin, W. Dankwort, E. Pitz, and S. Penselin, *Z. Physik* **200**, 467 (1967).
- ¹⁴P. A. Vanden Bout, E. Aygun, V. J. Ehlers, T. Incesu, A. Saplokoglu, and H. A. Shugart, *Phys. Rev.* **165**, 88 (1968).
- ¹⁵W. E. Blumberg, J. Eisinger, and M. P. Klein, *Phys. Rev.* **124**, 206 (1961).
- ¹⁶B. Smaller, *Phys. Rev.* **83**, 812 (1951).
- ¹⁷E. B. D. Lambe, Ph. D. thesis, Princeton University, 1959 (unpublished).
- ¹⁸L. C. Balling and F. M. Pipkin, *Phys. Rev.* **139**, A19 (1965); corrected by L. C. Balling, *Phys. Rev.* **163**, 114 (1967).
- ¹⁹O. Lutz, *Phys. Letters* **25A**, 440 (1967).
- ²⁰W. C. Dickinson, *Phys. Rev.* **80**, 563 (1950).
- ²¹G. Malli and S. Fraga, *Theoret. Chim. Acta* (Berlin) **5**, 275 (1966).
- ²²D. Ikenberry and T. P. Das, *J. Chem. Phys.* **43**, 2199 (1965).
- ²³T. Myint, D. Kleppner, N. F. Ramsey, and H. G. Robinson, *Phys. Rev. Letters* **17**, 405 (1966).
- ²⁴W. H. Parker, B. N. Taylor, and D. N. Langenberg, *Phys. Rev. Letters* **18**, 287 (1967).
- ²⁵R. G. Brewer, *J. Chem. Phys.* **38**, 3015 (1963).
- ²⁶J. P. Barrat and C. Cohen-Tannoudji, *Compt. Rend.* **252**, 394 (1961); J. P. Barrat and C. Cohen-Tannoudji, *J. Phys. Radium* **22**, 329, 443 (1961); C. Cohen-Tannoudji, *Ann. Phys. (Paris)* **7**, 423, 469 (1962).
- ²⁷M. Arditi and T. R. Carver, *Phys. Rev.* **124**, 800 (1961).
- ²⁸L. D. Schearer, *Phys. Rev.* **127**, 512 (1962).
- ²⁹C. Cohen-Tannoudji, *Compt. Rend.* **252**, 394 (1961).
- ³⁰C. Cohen-Tannoudji, *Compt. Rend.* **253**, (1961).
- ³¹F. Bloch and A. Siegert, *Phys. Rev.* **57**, 522 (1940).
- ³²R. Kubo, *Fluctuation, Relaxation, and Resonance in Magnetic Systems*, edited by D. Ter Haar (Oliver and Boyd, London, 1962), pp. 23-68.
- ³³E. M. Purcell, private communication.
- ³⁴See discussion by P. L. Bender, *Quantum Electronics III*, edited by P. Grivet and N. Bloembergen (Columbia University Press, New York, 1964), pp. 263-273.

Short-Range Effects on the Pressure Shift for a Nitrogen Atom in a Rare-Gas Atmosphere*

Supriya Ray and T. P. Das

Department of Physics, University of California, Riverside, California

(Received 1 May 1967; revised manuscript received 24 January 1968)

The short-range contribution to the pressure shift of the hyperfine constant has been analyzed for a nitrogen atom in interaction with a rare-gas atom, and specific calculations are performed for helium as buffer gas. Two mechanisms are found to contribute to the short-range shift; the first, due to the finite spin density at the nitrogen nucleus from the distorted $2p$ valence electrons, contributes only 1% of the experimental shift. The second mechanism arises from the exchange polarization of $1s$ and $2s$ cores by the perturbed valence electrons, and produces a shift of 0.76 cps/mm Hg, as compared to the experimental value of 0.27 cps/mm Hg. The results are in disagreement with earlier assumptions of a negligible short-range effect. Possible sources that could influence the theoretical value to improve agreement with experiment are discussed.

I. INTRODUCTION

Careful hyperfine pressure-shift measurements by the optical pumping technique¹ have so far been

carried out²⁻⁴ for hydrogen, nitrogen, phosphorus, and the alkali atoms in atmospheres of various rare gases. The experimental results for the hydrogen atom indicate that as one passes on to